

PAPER • OPEN ACCESS

## Structural, microstructural and optical property studies on sol-gel synthesized Cr/Fe-doped CuO nanoparticles

To cite this article: J Praveen Kumar *et al* 2020 *J. Phys.: Conf. Ser.* **1495** 012011

View the [article online](#) for updates and enhancements.



**IOP | ebooks™**

Bringing together innovative digital publishing with leading authors from the global scientific community.

Start exploring the collection—download the first chapter of every title for free.

# Structural, microstructural and optical property studies on sol-gel synthesized Cr/Fe-doped CuO nanoparticles

J Praveen Kumar<sup>1</sup>, K S K R Chandra Sekhar<sup>2</sup>, Anantharao Paila<sup>2</sup>, Kandula Kumara Raja<sup>3</sup>, B Suryanarayana<sup>2</sup> and Tirupathi Patri<sup>1\*</sup>

<sup>1</sup>Department of Physics, Rajiv Gandhi University of Knowledge Technologies, (AP-IIIT), RK Valley, Kadapa – 516330, India

<sup>2</sup>Department of Engineering Physics, A.U. College of Engineering (A), Andhra University, Visakhapatnam – 530003, India

<sup>3</sup>St. Martin's Engineering College, Dhullapally, Secunderabad - 500100, India

Email: ptirupathi36@gmail.com

**Abstract:** Here with we reported a detailed synthesis of Fe/Cr co-doped Copper oxide nanoparticles with a simple and inexpensive wet chemical method. The pure and Fe, Cr substituted CuO nanoparticles was prepared with sol-gel chemical method are expedient for industrial application. The preliminary X – ray diffraction and Rietveld refinement study revealed a pure crystallinity nature with monoclinic crystal with C2/c phase. The average crystallite size was calculated by Scherrer's formula in order of 21 nm and further observation indicates with increase concentration crystalline size increases. The scanning electron microscopy (SEM) images indicate particles are in 20-30 nm range. The Raman spectroscopic study indicates the existence of molecular groups in the CuO nanoparticles with the doping of Cr and Fe.

## 1. Introduction

From the time when the discovery of carbon nanotubes starts in 1991, since then one – dimensional (1D) nanomaterials have concerned significant attention owing to their wide variety physical and chemical properties such as optical, electrical and magnetic properties and their applications in nanodevices [1]. In special attention was paid in nano-sized metal oxides with controlled morphology, structure and size gained significant technological and scientific interest because of large surface area to volume ratio of nano-structures [2,3]. Cutting-edge single phase transition metal oxide materials owing to their wide and tunable band gap with it is cost effective, ease fabrication and nonhazardous in nature. Nevertheless, low dimensional transition metal oxides like ZnO, TiO<sub>2</sub>, SnO<sub>2</sub> and CuO are being researched for microelectronics, gas sensing and photovoltaic and wide industry applications.

Among all reported metal oxides, CuO is the least studied in spite of controlling the oxidation state and growth kinetics of copper during synthesis that prominently affect its physical and chemical properties. The contemporary studies have shown that copper oxide-based nanoparticles (NPs), in the form of cupric oxide (CuO) and cuprous oxide (Cu<sub>2</sub>O) in precise, are industrially important materials that can be broadly used in applications, such as magnetic storage media, solar energy transformation, gas sensors, anode electrodes for batteries, electrical contacts in nanoelectronics, multiferroic, superconductors and catalysts [2–8]. In point of multiferroic nature i.e., occurrence of ferroelectric and magnetic property in single phase CuO metal oxides, we synthesized CuO nanoparticles by sol-gel method. Along with dopant of Fe and Cr doped CuO particle also consider to be the multiferroic



nature. In present paper, we reported structural, microstructural and optical properties of CuO, Fe/Cr doped CuO nanoparticle.

## 2. Experimental Procedure

The pure and doped CuO nanoparticle were synthesized in sol – gel method, with help of precursor solution of ethylene glycol and citric acid [ $C_6H_8O_7$ ] with in 1:1 ratio a precursor solution was prepared in a deionized (DI) water. Formerly Copper nitrate trihydrate [ $Cu(NO_3)_2 \cdot 3H_2O$ ], Chromium nitrate nonahydrate [ $Cr(NO_3)_3 \cdot 9H_2O$ ] and Iron nitrate nonahydrate [ $Fe(NO_3)_3 \cdot 9H_2O$ ] was dissolved in equal ratios of deionized (DI) water of as solvent. A continuous stirring of solution with 3 – 4 hours at 50 °C, a green solution was acquired. The homogeneous mixture was maintained under reflux at 130 – 150 °C for 8 hours. A wet-gel was attained after the evaporation of excess solvents. And then finally, a powder was calcined at 500 °C for 5hour and then grinded. The X-ray diffraction was conducted on a Philips Analytical X'PERT diffractometer using a Cu  $K\alpha$  radiation ( $\lambda = 1.54056 \text{ \AA}$ ) in range  $2\theta$  20° to 80°. Further, Phase analysis was carried by FullProf software. Particle morphology and size distribution was estimated using the micrographs collected on a scanning electron microscope (model: Supra SEM Zeiss). Phonon modes variation was also determined by the analysis of the Raman spectrum collected with incident green LASER wavelength of 488 nm.

## 3. Results And Discussion

### 3.1. X-Ray Diffraction study by using Rietveld refinement

The crystalline property and particle size information was carried out by using X-ray diffraction technique. The typical XRD patterns of pure CuO and Cr, Fe doped CuO nanoparticles annealed at 600°C is shown in Figure 1. It is clear from Fig 1 that all samples exhibit the monoclinic structure. No other impurity peaks were observed in the XRD pattern, indicating a single-phase sample formation of CuO nanoparticles. Furthermore, Fe, Cr and Fe/Cr-doped CuO nanoparticle x-ray diffraction patter also represented in Figure 1. It is clearly showing a sharp rise in maximum peak intensity with increasing Fe or/and Cr in CuO. On the other hand, Fe/Cr-co-doped sample shows sudden decreasing maximum peak intensity, without any other detectable impurity peaks. The lattice parameters are manifest to explain the structural stability with the substitution of Fe and Cr in CuO shown in Figure 4b. The crystallite size was calculated using Scherrer formula,  $D=0.9\lambda/\beta\cos\theta$ , where  $\lambda$  is the wavelength of X-ray radiation,  $\beta$  is the full width at half maximum (FWHM) of the peaks at the diffracting angle  $\theta$ .

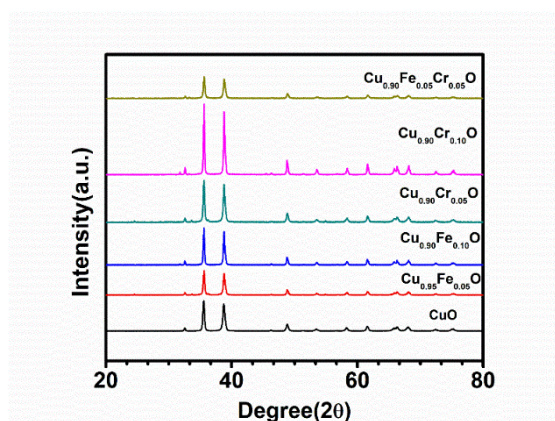


**FIGURE 1.** Evaluation of X – ray diffraction pattern of CuO,  $Cu_{0.95}Fe_{0.05}O$ ,  $Cu_{0.90}Fe_{0.10}O$ ,  $Cu_{0.95}Cr_{0.05}O$ ,  $Cu_{0.90}Fe_{0.10}O$  and  $Cu_{0.90}Fe_{0.05}Cr_{0.05}O$ .

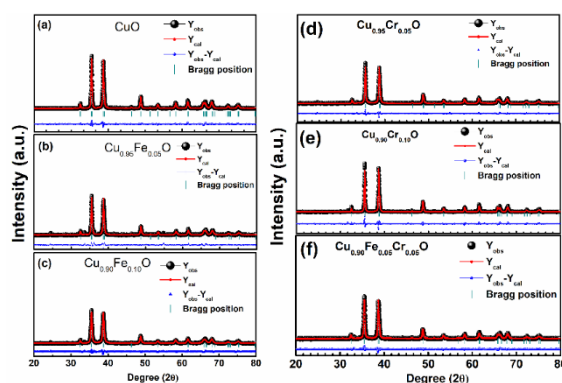


**FIGURE 2.** Rietveld refined XRD plots of CuO and Cr and Fe doped CuO nanoparticles (a) CuO; (b)  $Cu_{0.95}Fe_{0.05}O$ ; (c)  $Cu_{0.90}Fe_{0.10}O$ ; (d)  $Cu_{0.95}Cr_{0.05}O$ , (e)  $Cu_{0.90}Cr_{0.10}O$ , (f)  $Cu_{0.90}Fe_{0.05}Cr_{0.05}O$ .

Crystallite size, increases with dopant was observed, which is in the order of 20 to 30 nm range which was shown in Figure 4a at various concentrations in CuO. Furthermore, a clear shift in peak position of Fe, Cr and Cr Fe doped CuO nanoparticles towards larger angles, which indicates a slight distortion in the symmetry of the system due to the creation of vacancies and defects in the system. Defects generated in the system can be attributed to the charge imbalance occurs from Cr and Fe. In order to explore the possibility existing structural phase contribution of these nanoparticles, we consider Rietveld refinement by using FullProf software. It is well reported the room temperature structure of CuO has been argued to possess a stable monoclinic with  $C2/c$  ( $C_{2h}^6$ ) model. Keeping this in mind, we started considering  $C2/c$  space group initially to investigate crystal system. CuO and Fe/Cr-doped CuO nanoparticle XRD pattern was well fitted with monoclinic  $C2/c$  space group is shown in Figure 2(a-f) with reduced chi square ( $\chi^2$ ) values 2.56, 1.83, 2.9, 2.75, 4.29 and 2.28 for undoped CuO and also Fe 0.05, Fe 0.10, Cr0.05, Cr 0.10 and Fe0.05 Cr0.05 Respectively. The variation particles size, lattice parameters also shown in Fig. 4(a-b). The observed lattice parameters are slightly increased with the increase in dopant concentration might be the mismatch in ionic radii of  $Fe^{3+}/Cr^{3+}$  at Cu site.

### 3.2. Raman Spectroscopic studies

Raman spectroscopy, which is a sensitive probe to the local atomic arrangements and vibrations of the materials, has been widely used to investigate the microstructural nature of the nanosized materials [9,10]. Recently, much work has been done on the Raman spectra of semiconductor nanocrystals. Figure 3(a-d) shows the Raman spectra of CuO and Fe, Cr doped CuO nanoparticles with different shuttle-like morphologies. One can find that the Raman spectra exhibit three main one-phonon modes at 282, 337 and 613  $cm^{-1}$ , respectively. The peak at 282  $cm^{-1}$  can be assigned to the  $A_g$  mode, while the peaks at 337 and 613  $cm^{-1}$  can be assigned to the  $B_g$  modes. In addition to three main one-phonon Raman scattering peaks, one also can find a broadened peak at 1130  $cm^{-1}$ , which is assigned to multi-phonon (MP) transition for the case of the MP band, one can easily find from the Raman spectra in Figure 3(a-d) that the MP intensity varies with morphology and the size of the as-prepared CuO nanostructures. These observations clearly suggest an appearance of nanostructure monoclinic crystal structure.

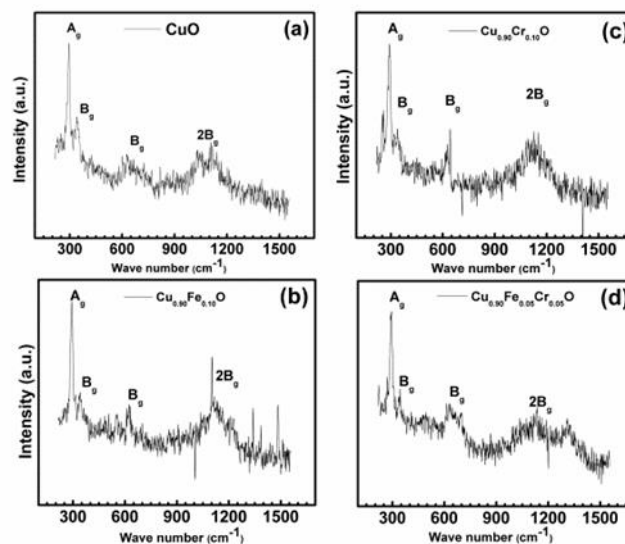


**FIGURE 3.** Raman spectra of CuO, Cr and Fe doped CuO. (a) CuO (b)  $Cu_{0.90}Fe_{0.10}O$  (c)  $Cu_{0.90}Cr_{0.10}O$  (d)  $Cu_{0.90}Fe_{0.05}Cr_{0.05}O$

### 3.3. Surface morphology studies

Figure 4(c-d) shows the SEM micrographs of calcined powder of CuO and Fe/Cr-co-doped CuO nanoparticles. It is clearly showing the calcined powder particles are spherical in shape and



nonuniform distribution. The average particles size was calculated by using histogram which were shown in Figure 4(e-f), which are  $0.72 \mu\text{m}$  and  $0.4 \mu\text{m}$  for CuO and  $\text{Cu}_{0.90}\text{Fe}_{0.10}\text{O}$ . Further, the particle size increases with increasing dopant concentration.

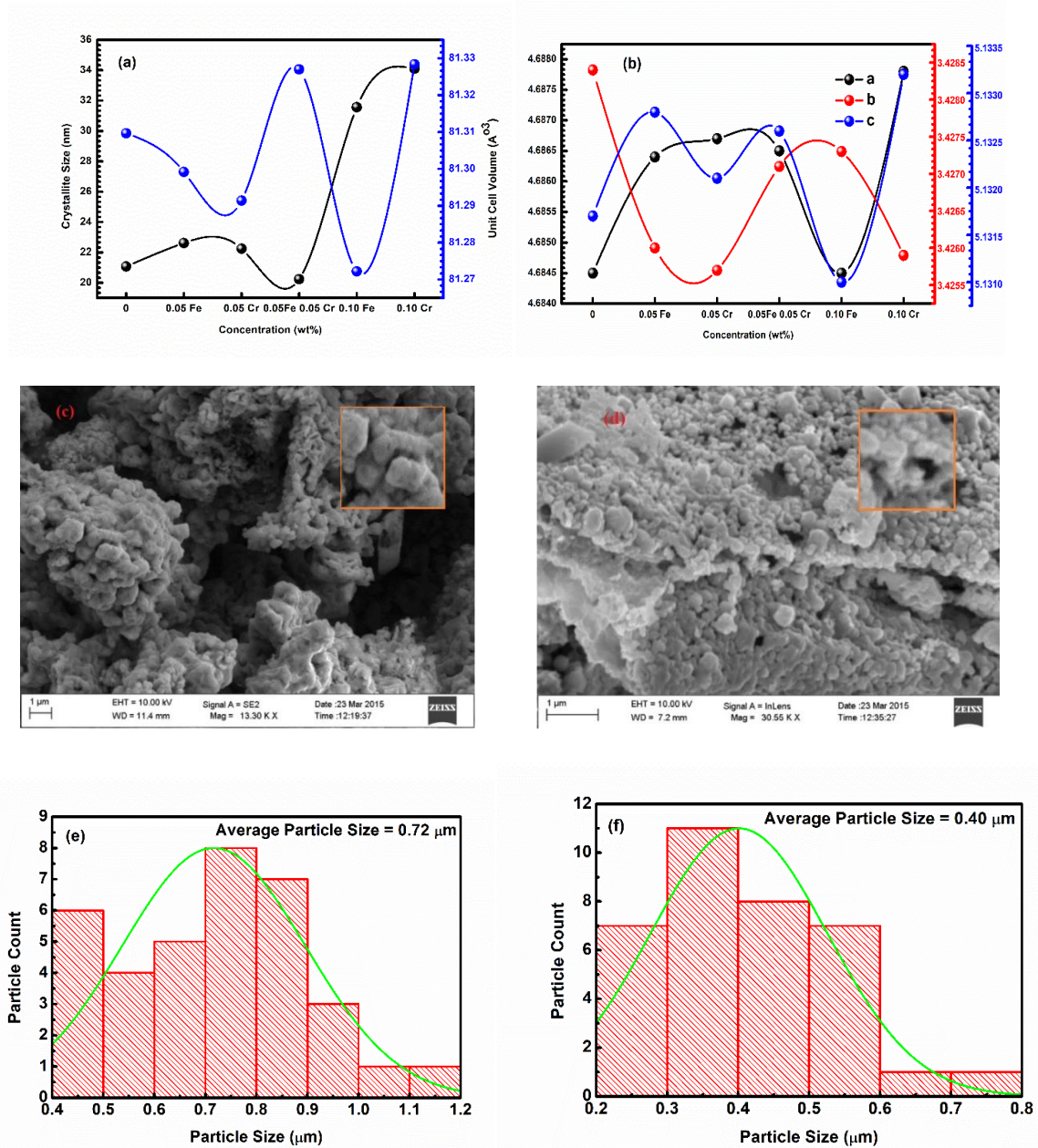


**FIGURE 4.** (a) Evaluation of Crystallite size, volume of the unit cell and variation of lattice parameters (a, b and c) with the concentration of Fe and Cr in CuO. (b) Dependence of lattice parameters a, b and c ( $\text{\AA}$ ) on concentration of Fe and Cr in CuO. (c – d) Typical Scanning electron microscopy images of CuO and  $\text{Cu}_{0.90}\text{Fe}_{0.10}\text{O}$  respectively. And (e – f) Histograms illustrating the Particle size variation for CuO and  $\text{Cu}_{0.90}\text{Fe}_{0.10}\text{O}$  respectively.

#### 4. Conclusions

In Summary, we have selectively synthesized CuO nano particles along with doped Fe, Cr by Sol – gel method. The X-ray diffraction study shows phase purity with crystalline nature. The Rietveld refinement technique shows carried the structural phase transitions single-phase monoclinic with C2/c phase for all doped CuO nanoparticles. Further, local atomic structure and existence phase purity confirmed by Raman Spectroscopy. Particle size and surface morphology of calcined powder along with sintered pellets were also reported in detailed.

#### Acknowledgements

The authors would like to thank UGC-DAE Consortium, Mumbai Centre, India for providing experimental facilities and financial support under UGC-DAE, CRS-M-216-Sponsored Project Scheme.

#### References

- [1] F. Weyland, M. Acosta, M. Vögler, Y. Ehara, J. Rödel, N. Novak, Electric field–temperature phase diagram of sodium bismuth titanate-based relaxor ferroelectrics, *J. Mater. Sci.* 53 (2018). doi:10.1007/s10853-018-2232-5.
- [2] K. Zhang, C. Rossi, C. Tenaillon, P. Alphonse, J.Y. Chane-Ching, Synthesis of large-area and aligned copper oxide nanowires from copper thin film on silicon substrate, *Nanotechnology*. 18 (2007). doi:10.1088/0957-4484/18/27/275607.
- [3] M. Cao, C. Hu, Y. Wang, Y. Guo, C. Guo, E. Wang, A controllable synthetic route to Cu, Cu<sub>2</sub>O, and CuO nanotubes and nanorods Electronic supplementary information (ESI) available: EDS patterns of nanotubes and SEM images of nanorods. See <http://www.rsc.org/suppdata/cc/b3/b304505f/>, *Chem. Commun.* 1 (2003) 1884. doi:10.1039/b304505f.
- [4] Y.S. Cho, Y.D. Huh, CuO nanotubes synthesized by the thermal oxidation of Cu nanowires, *Bull. Korean Chem. Soc.* 29 (2008) 2525–2527. doi:10.5012/bkcs.2008.29.12.2525.
- [5] G. Malandrino, S.T. Finocchiaro, R. Lo Nigro, C. Bongiorno, C. Spinella, I.L. Fragalà, Free-standing copper(II) oxide nanotube arrays through an MOCVD template process, *Chem. Mater.* 16 (2004) 5559–5561. doi:10.1021/cm048685f.
- [6] K. Karthik, N. Victor Jaya, M. Kanagaraj, S. Arumugam, Temperature-dependent magnetic anomalies of CuO nanoparticles, *Solid State Commun.* 151 (2011) 564–568. doi:10.1016/j.ssc.2011.01.008.
- [7] J.B. Reitz, E.I. Solomon, *PropyleneOxidationByCuoxide.pdf*, (1998) 11467–11478.
- [8] Y. Feng, X. Zheng, Plasma-enhanced catalytic CuO nanowires for CO oxidation, *Nano Lett.* 10 (2010) 4762–4766. doi:10.1021/nl1034545.
- [9] J. Suchanicz, I. Jankowska-Sumara, T. V. Kruzina, Raman and infrared spectroscopy of Na<sub>0.5</sub>Bi<sub>0.5</sub>TiO<sub>3</sub> - BaTiO<sub>3</sub> ceramics, *J. Electroceramics.* 27 (2011) 45–50. doi:10.1007/s10832-011-9648-5.
- [10] S.A. Nasser, Infrared absorption of some perovskite type titanates containing some additives, *J. Mater. Sci. Lett.* 9 (1990) 1453–1455. doi:10.1007/BF00721613.